Dependence of LC VCO Oscillation Frequency on Bias Current

Ting Wu, Un-Ku Moon, and Kartikeya Mayaram
School of Electrical Engineering and Computer Science
Oregon State University, 1148 KEC, Corvallis, OR 97331

Abstract – **LC-tuned voltage controlled oscillators (LC VCOs) are widely used in high performance phase locked loops (PLLs) and frequency synthesizers due to their high spectral purity. The oscillation frequency of an LC VCO is commonly assumed to be the resonant frequency of the LC tank. However, this is not accurate as shown in this paper. The oscillation frequency is also affected by the bias current. By applying our analysis to the Hegazi and Abidi's LC VCO, we propose a new digital trimming technique which can compensate for process variations and improve the phase noise performance.**

I. INTRODUCTION

To sustain oscillations, an oscillator must satisfy the Barkhausen criteria. Namely, for a positive feedback system, oscillations will occur when the loop gain has a zero phase shift with a magnitude of one at the oscillation frequency. In a practical oscillator the startup loop-gain magnitude should be greater than one in order for oscillations to build up to the steady-state amplitude that is limited by other nonlinear effects.

Fig. 1(a) shows a high-level oscillator schematic, where Y denotes a resonator admittance and $Y_{(-)}$ denotes a negative admittance that compensates for the energy losses in the resonator.

$$Y = G + jB \tag{1}$$

$$Y_{(-)} = G_{(-)} + jB_{(-)} \tag{2}$$

In the steady state of an oscillator, the phase condition requires that the loop phase shift is zero. As a consequence,

$$B_{(-)} + B = 0 \tag{3}$$

The oscillation frequency of a LC VCO, ω_{OSC}, is commonly assumed to be the resonant frequency ω_0, expressed by (4). However, this is not accurate in practical circuits [1] because of energy losses in the resonator inductor and capacitor.

$$\omega_{OSC} = \omega_0 = \frac{1}{\sqrt{LC}} \tag{4}$$

To understand this, a simplified model of a LC oscillator is shown in Fig. 1(b), where R_L and R_C represent the series losses of the inductor (L) and capacitor (C), respectively.

The admittance of the resonator is

$$Y = \frac{1}{j\omega L + R_L} + \frac{1}{1/(j\omega C) + R_C} = G + jB \tag{5}$$

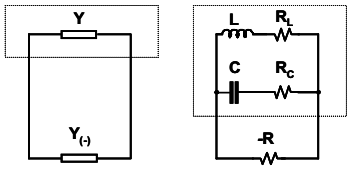

Fig. 1. (a) A general oscillator model. (b) A model of LC-tank oscillator.

where G and B are

$$G = \frac{R_L}{R_L^2 + \omega^2 L^2} + \frac{R_C}{R_C^2 + 1/(\omega^2 C^2)} \tag{6}$$

$$B = \frac{-\omega L}{R_L^2 + \omega^2 L^2} + \frac{1/(\omega C)}{R_C^2 + 1/(\omega^2 C^2)}$$

If the LC oscillator is connected to a pure negative resistor ($-R$), then $B_{(-)}$ is zero. From the phase condition (3), B must also equal to zero.

$$B = \frac{\omega C}{1 + 1/Q_C^2} - \frac{1/\omega L}{1 + 1/Q_L^2} = 0 \tag{7}$$

where Q_C and Q_L are the quality factors of the capacitor and the inductor, respectively. These are defined by

$$Q_L = \omega L / R_L \qquad Q_C = 1/\omega C R_C \tag{8}$$

Assume that both Q_C and Q_L are much larger than 1. Then it can be shown that

$$\omega^2 LC = (1 + \frac{1}{Q_C^2}) \Big/ (1 + \frac{1}{Q_L^2}) \approx 1 + \frac{1}{Q_C^2} - \frac{1}{Q_L^2} \tag{9}$$

The relationship of the oscillation frequency ω_{OSC} to the resonant frequency ω_0 is

$$\omega_{OSC}^2 \approx \omega_0^2 (1 - \frac{1}{Q_L^2} + \frac{1}{Q_C^2}) \tag{10}$$

In other words, the oscillation frequency deviates from the resonant frequency due to the losses in the inductor and capacitor. The energy loss in the inductive branch causes the oscillation frequency to decrease, while the loss in capacitive branch causes the oscillation frequency to increase [1].

II. BIAS CURRENT DEPENDENCE OF LC VCO

Cross-coupled transistors are commonly used to produce a negative impedance in differential LC VCOs. Shown in Fig. 2(a) is a NMOS cross-coupled pair.

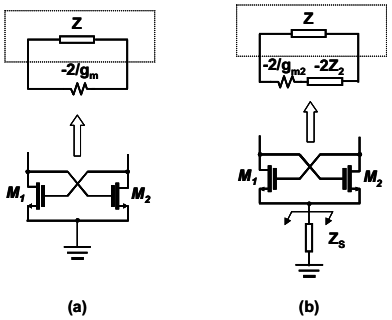

Fig. 2. Negative impedances stem from the cross-coupled transistors. (a) At DC. (b) At high frequencies.

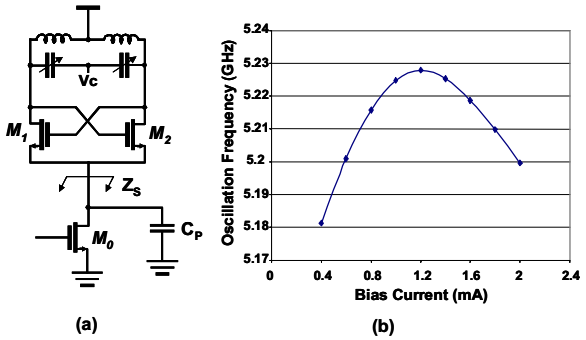

Fig. 3. (a) Schematic of a LC VCO. (b) Simulated oscillation frequency of this VCO vs. bias current.

This cross-coupled transistor pair creates a negative impedance ($-2/g_m$) across the resonator, where g_m is the transconductance of the NMOS transistor. This is true only at low frequency. At high frequencies, an impedance Z_S is seen by the source node of the cross-coupled transistors, as shown in Fig. 2(b). Transistor current at even harmonics (where the 2nd harmonic component is dominant) sinks into the source impedance Z_S. It can be shown that, at the 2nd harmonic frequency, the equivalent impedance seen by the resonator is ($-2/g_{m2}-2Z_2$), where g_{m2} and Z_2 denote the NMOS transconductance g_m and the source impedance Z_S at the 2nd harmonic frequency.

For example, Fig. 3(a) shows the schematic of a commonly used LC VCO, where M0 is a tail current source transistor, and M1 and M2 are cross-coupled transistors. The resonator consists of inductors and varactors. As explained above, the total negative impedances associated with the cross-coupled transistors include a DC component and a 2nd harmonic component. At the 2nd harmonic frequency, the source impedance Z_S is given by

$$Z_S\Big|_{2^{nd}\,harmonic} = Z_2 = 1/(j2\omega_{OSC}C_P) \approx 1/(j2\omega_0 C_P) = Z_{20} \qquad (11)$$

where C_P denotes the total capacitance at the source node of the cross-coupled transistors, including the source capacitance of M1 and M2, the drain capacitance of M0 and the parasitic capacitance at the source node. Using this information, one can obtain

$$B_{(-)} = \frac{-\omega_{OSC}C_P}{1+4\omega_{OSC}{}^2 C_P{}^2/g_{m2}{}^2} = \frac{-\omega_{OSC}C_P}{1+1/(g_{m2}{}^2|Z_2|^2)} \approx \frac{-\omega_0 C_P}{1+1/(g_{m2}{}^2|Z_{20}|^2)} \qquad (12)$$

The phase condition of (3) yields

$$B + B_{(-)} = \frac{\omega C}{1+1/Q_C{}^2} - \frac{1/\omega L}{1+1/Q_L{}^2} + \frac{-a_0 C_P}{1+1/(g_{m2}{}^2|Z_{20}|^2)} = 0 \qquad (13)$$

Similar to the derivation in Section I, it can be shown that the oscillation frequency is a function of the source node capacitance C_P and the transconductance g_{m2}, as given by

$$\omega_{OSC}{}^2 \approx \omega_0{}^2\left(1-\frac{1}{Q_L{}^2}+\frac{1}{Q_C{}^2}+\frac{C_P}{C}\left(1-\frac{1}{g_{m2}{}^2|Z_{20}|^2}\right)\right) \qquad (14)$$

Therefore, the source node capacitance C_P causes the oscillation frequency to increase. Furthermore, since g_{m2} increases with an increase in the bias current, (14) implies that the oscillation frequency of this LC VCO also increases with an increase in the bias current.

The oscillation frequency variation due to the source node capacitance C_P can also be explained as follows. The cross-coupled transistors effectively transfer the source node capacitance as a negative capacitance that is seen by the resonator. For narrowband applications, this negative capacitor can be considered as an equivalent inductor [2]. If we define this equivalent inductor as L_E and its quality factor as Q_E, then

$$B_{(-)} = \frac{-\omega_{OSC}C_P}{1+4\omega_{OSC}{}^2 C_P{}^2/g_{m2}{}^2} = \frac{-1/\omega_{OSC}L_E}{1+1/Q_E{}^2} \qquad (15)$$

from which we obtain

$$L_E = 1/C_P\omega_{OSC}{}^2 \quad , \quad Q_E = g_{m2}{}^2/4C_P{}^2\omega_{OSC}{}^2 \qquad (16)$$

Equivalently, an additional inductor L_E is connected in parallel with the original resonator. The total inductance is then reduced, resulting in an increased frequency of oscillation. Since Q_E increases with an increase in g_{m2} (bias current), (10) suggests that the oscillation frequency also increases with an increase in bias current.

To verify our analysis, we have designed and simulated a LC VCO employing the topology in Fig. 3(a) in a 0.18μm CMOS technology with a 1V supply voltage. The simulated oscillation frequency as a function of the bias current is shown in Fig. 3(b). As expected, for small bias currents, the oscillation frequency increases with an increase in the bias current.

When the bias current is larger than 1.2mA the oscillation frequency drops with an increase in the bias current. This discrepancy exists because our analysis does not account for harmonics in the oscillator waveform. The active devices in an oscillator drive the resonator with a harmonic-rich waveform, which also changes the oscillation frequency [1]. In fact, the oscillation frequency will decrease in order to ensure that the energy is balanced between the inductor and the capacitor [1, 2]. Consequently, the oscillation frequency is altered due to two effects. When the bias current is large, the frequency variation due to harmonic distortion is dominant, causing the oscillation frequency to drop.

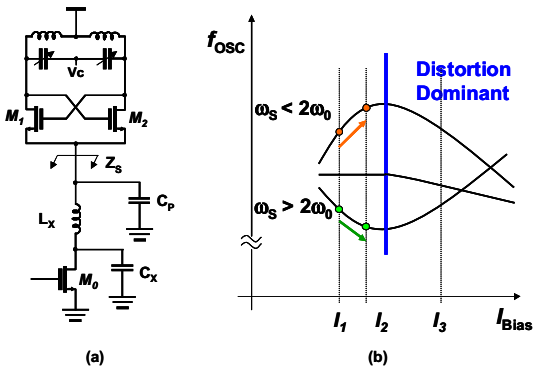

Fig. 4. (a) Hegazi and Abidi's LC VCO [3]. (b) Relationship between the oscillation frequency and the bias current for the VCO in (a).

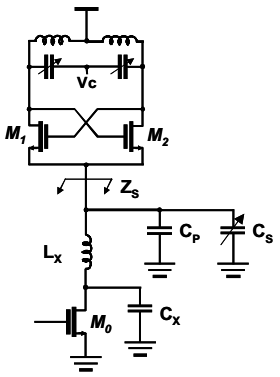

Fig. 5. LC VCO with a digitally controlled capacitor C_S [5].

III. OSILLATION FREQUENCY OF HEGAZI and ABIDI'S LC VCO

In this section, we study the bias current dependence of the oscillation frequency in Hegazi and Abidi's VCO [3], which is shown in Fig. 4 (a).

This VCO is a modified version of the VCO in Fig. 3 (a). A large capacitor with a value of C_X (tens of pico farads) is inserted in parallel with M0 to filter the tail transistor noise. Nevertheless, C_X also adds an additional loading on the resonator, as discussed earlier. The quality factor of the additional equivalent inductor is small if C_X is large, as suggested by (16).

To address the loading problem, an inductor with a value of L_X is inserted between the drain of the tail transistor M0 and the source node of the cross-coupled transistors [3]. Let us define the resonant frequency caused by the inductance L_X and the total capacitance at the source node C_P to be ω_S. If the value of L_X is chosen properly such that ω_S is close to the 2nd harmonic frequency of the oscillator, then the source impedance Z_S seen by the cross-coupled transistors is nearly infinity at the 2nd harmonic frequency. This can be shown mathematically. Given that C_X is much larger than C_P, the impedance Z_S is approximately given by

$$Z_S\big|_{2^{nd}\,harmonic} = Z_2 \approx \frac{j(2\omega_{OSC})L_X}{1-(2\omega_{OSC})^2/\omega_S^2} \approx \frac{j(2\omega_0)L_X}{1-(2\omega_0)^2/\omega_S^2} = Z_{20} \quad (15)$$

where the resonant frequency ω_S is

$$\omega_S = \frac{1}{\sqrt{L_X C_P}} \approx 2\omega_{OSC} \quad (16)$$

As can be seen from (15), when the resonant frequency ω_S is approximately the 2nd harmonic frequency, the impedance Z_S approaches infinity.

In order to obtain the oscillation frequency of this VCO, $B_{(-)}$ is derived and is given in (17). The oscillation frequency can be then expressed by (18).

$$B_{(-)} \approx \frac{1-(2\omega_{OSC})^2/\omega_S^2}{4\omega_{OSC}L_X(1+1/g_{m2}^2|Z_{20}|^2)} \quad (17)$$

$$\omega_{OSC}^2 \approx \omega_0^2\left(\left(1-\frac{1}{Q_L^2}+\frac{1}{Q_C^2}\right)-\frac{L}{4L_X}\left(1-\frac{(2\omega_{OSC})^2}{\omega_S^2}\right)\left(1-\frac{1}{g_{m2}^2|Z_{20}|^2}\right)\right) \quad (18)$$

Equation (18) shows that the oscillation frequency is again a function of the bias current, through the dependence on g_{m2}.

Another important point to note is that, the oscillation frequency is also affected by the resonant frequency ω_S. Depending on the polarity of the term $(1-(2\omega_{OSC})^2/\omega_S^2)$ the oscillation frequency can either increase or decrease with an increase in the bias current. For example, if ω_S is smaller than $2\omega_{OSC}$, $(1-(2\omega_{OSC})^2/\omega_S^2)$ is negative and hence the oscillation frequency will increase with an increase in the bias current. On the other hand, if ω_S is larger than $2\omega_{OSC}$, $(1-(2\omega_{OSC})^2/\omega_S^2)$ is positive and hence the oscillation frequency will decrease with an increase in the bias current. If ω_S is equal to $2\omega_{OSC}$, the term $(1-(2\omega_{OSC})^2/\omega_S^2)$ is zero. Thus, the oscillation frequency is independent of the bias current when ω_S is equal to $2\omega_{OSC}$.

Once again the analysis above is only valid for small bias currents. At large bias currents, distortion effects become important. Simulations show that, when ω_S is smaller than $2\omega_{OSC}$, the oscillation frequency increases for small bias currents but drops at larger bias currents. Conversely, when ω_S is larger than $2\omega_{OSC}$, the oscillation frequency drops for small bias currents but can increase at larger bias currents. This relationship between the oscillation frequency of the Hegazi and Abidi's LC VCO and the bias current is shown in Fig. 4 (b).

IV. DIGITAL TRIMMING TECHNIQUE

Although the Hegazi and Abidi's VCO was able to achieve low phase noise performance [3], two obstacles need to be addressed in practical implementations. First, the VCO only works optimally at a particular oscillation frequency. At other frequencies the 2nd harmonic frequency is altered but the resonant frequency ω_S is unchanged. Simulation results show that the phase noise performance is significantly degraded if the resonant frequency ω_S is different from the 2nd harmonic frequency $2\omega_{OSC}$. This observation was also confirmed in [4], where a close-in

phase noise difference of 10dB was measured when the VCO was tuned from 725MHz to 806MHz in Hegazi and Abidi's VCO. To reduce this problem, a digitally controlled capacitor C_S can be added in parallel with the capacitor C_P [5], as shown in Fig. 5. By doing so, it is feasible to change the resonant frequency ω_s, and thus track the change of the oscillation frequency.

One remaining obstacle is that the inductance L_X and the capacitance C_P are very difficult to estimate due to process variations. As a result, it is difficult to achieve the optimal phase noise performance. To resolve this problem, we propose a trimming technique to ensure that the resonant frequency ω_s is equal to the 2nd harmonic frequency of the VCO.

As discussed in Section III, for small bias currents, the oscillation frequency variation due to bias current is dependent on ω_s, i.e., the total capacitance C_P+C_S. This observation can be used in our trimming technique. As indicated in Fig. 4(b), bias currents I_1 and I_2 are small but I_3 is large. When the bias current is changed from I_1 to I_2, if the oscillation frequency increases, then we know that ω_s is smaller than $2\omega_{OSC}$. The capacitance C_S should be reduced. On the other hand, if the oscillation frequency decreases when the bias current is changed from I_1 to I_2, then ω_s is larger than $2\omega_{OSC}$ and the capacitance C_S should be increased. This trimming procedure should be continued until the condition $f_{OSC}\big|_{I_1} = f_{OSC}\big|_{I_2}$ is met. After the capacitor C_S is trimmed, a large bias current, say I_3, should be used in the VCO to increase the output amplitude for a better phase noise performance.

To demonstrate our proposed trimming technique, we have designed and simulated the LC VCO of Fig. 5 in a 0.18µm CMOS technology with a 1V supply voltage. The value of L_X is 0.75nH. A 5-bit digitally controlled capacitor C_S is used with the least significant bit (LSB) value of 10fF. The simulated oscillation frequency as a function of the bias current for different C_S is given in Fig. 6 (only 5 results with different codes for C_S are shown). The code of "01110" corresponds to the optimum code, at which the total capacitance C_P+C_S is resonant with the inductance L_X at $2\omega_{OSC}$. The codes of "00100" and "01001" correspond to a smaller C_S than the optimum value (ω_s larger than $2\omega_{OSC}$) while the codes of "10011" and "11000" correspond to a larger C_S than the optimum value (ω_s smaller than $2\omega_{OSC}$). As shown in Fig. 6, for bias currents from 0.5mA to 1.0mA, the variation of the oscillation frequency behaves the same way as predicted by our analysis.

The simulated phase noise at both 50kHz offset and 1MHz offset for different C_S is summarized in Fig. 7. A 4mA bias current is used for each simulation. When using the optimum code "01110" the phase noise is much better than those with other codes. This indicates that our proposed trimming technique can have a significant impact on the overall performance of the oscillator.

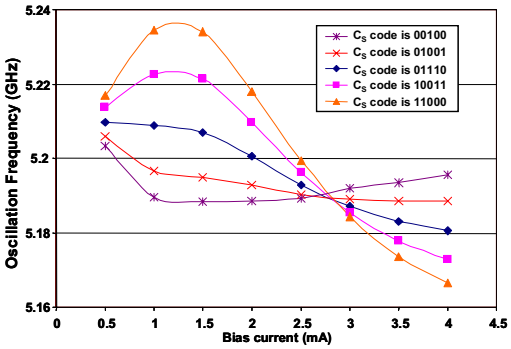

Fig. 6. Simulated oscillation frequency of the VCO in Fig. 5 vs. the bias current for different C_S.

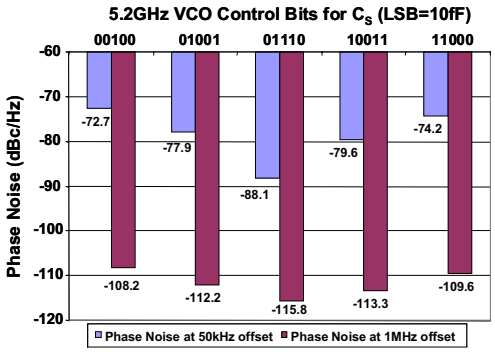

Fig. 7. Simulated phase noise of the 5.2GHz VCO in Fig. 5 using a 4mA bias current for different C_S.

V. CONCLUSIONS

In this paper, the bias current dependence of the oscillation frequency of a differential LC VCO is described. Simulation results validate our analysis. With the aid of our analysis, we have proposed a digital trimming technique to optimize phase noise performance of Hegazi and Abidi's LC VCO. An improvement in the phase noise of 3dB at 1MHz offset and 10dB at 50kHz offset can be achieved.

ACKNOWLEDGMENT

This work is supported by the Semiconductor Research Corporation under contract 2003-HJ-1076.

REFERENCES

[1] J. Groszkowski, *Frequency of Self-Oscillations*. Oxford, Pergamon Press, 1964.

[2] J. J. Rael and A. Abidi, "Physical processes of phase noise in differential LC oscillators," in *Custom Integrated Circuits Conf.*, pp. 569-572, May 2000.

[3] E. Hegazi, H. Sjoland, and A. Abidi, "A filtering technique to lower oscillator phase noise," in *Dig. Tech. Papers IEEE ISSCC*, pp. 364-365, Feb. 2001.

[4] K. Hoshino, E. Hegazi, J. Rael, and A. Abidi, "A 1.5V, 1.7mA 700MHz CMOS LC oscillator with no upconverted flicker noise," in *Proc. of the European Solid State Circuits Conference*, pp. 337-340, Sep. 2001.

[5] E. Hegazi and A. Abidi, "A 17-mW transmitter and frequency synthesizer for 900-MHz GSM fully integrated in 0.35-µm CMOS," *IEEE Journal of Solid-State Circuits*, vol.38, pp. 782-792, May 2003.